Step-induced deconstruction and step-height evolution of the Au(110) surface

U. Romahn
Kernforschungszentrum Karlsruhe G.m.b.H., Institut für Nukleare Festkörperphysik, Postfach 3640, 7500 Karlsruhe 1, Germany

P. von Blanckenhagen
Kernforschungszentrum Karlsruhe G.m.b.H., Institut für Materialforschung I, Postfach 3640, 7500 Karlsruhe 1, Germany

C. Kroll and W. Göpel
Institut für Physikalische und Theoretische Chemie der Universität, Auf der Morgenstelle 8, 7400 Tübingen, Germany
(Received 27 January 1992; revised manuscript received 12 October 1992)

We use temperature-dependent high-resolution low-energy electron diffraction and spot-profile analysis low-energy electron diffraction to study the Au(110) surface at room temperature up to 786 K. The experimental data were analyzed within the framework of the kinematic theory. Oscillations were determined of the positions of half order and fundamental Bragg peaks as well as of the full width at half maximum of the specular peak as a function of perpendicular momentum transfer. Evidence of monoatomic steps occurring in the [001] direction was found below and around the $(2\times1)\rightarrow(1\times1)$ transition at T_c. Above T_c, the surface gets smoother in the [001] direction; at the roughening temperature, T_R, the evolution of multiple-height steps starts in both symmetry directions.

I. INTRODUCTION

In recent years, the (110) surface of Au has been of great interest because of multilayer relaxation, reconstruction, deconstruction, roughening, and premelting. At low temperature, this surface spontaneously forms a (2×1) missing-row reconstruction.[1–3] At a certain critical temperature T_c it undergoes a deconstruction transition.[1–12] In Fig. 1 the cross section of the fcc(110)(2×1) surface is shown with steps and domain walls, which also appears spontaneously on the Pt(110) surface.

Earlier investigations furnished evidence of the deconstruction transition on these surfaces being in the two-dimensional (2D) Ising universality class.[2,13,14] At or above T_c, these surfaces are expected to show a Kosterlitz-Thouless- (KT) type roughening transition.[14–18] For the Pt(110) surface, Robinson, Vlieg, and Kern[10] discussed their x-ray-diffraction results of deconstruction within the framework of a roughening-induced deconstruction transition. That description is in contrast to a model proposed by Villain and Vilfan,[14] although the critical exponents for the Pt(110) deconstruction transition as deduced from the temperature dependence of the intensity and the full width at half maximum (FWHM) of a half-order peak are in good agreement with the theoretical 2D Ising exponent.[19] In a detailed low-energy electron-diffraction (LEED) study of the critical behavior of the deconstruction transition on the Au(110) surface, Compuzano *et al.*[13] derived critical exponents in agreement also with the 2D Ising model, but the authors offered no possible mechanism responsible for that transition.

In theoretical studies of the reconstructed fcc(110) surfaces[14–18,20] various mechanisms have been discussed which might account for the deconstruction transition and the role of steps in that transition. Villain and Vilfan[14] predicted a deconstruction transition within a 2D Ising model and found a roughening transition occurring at a temperature T_R, approximately 100 K above T_c. Deconstruction should be initiated by the creation of domains with different structures [(2×1) and (1×1)] causing domain walls (antiphase boundaries). Simple energetic arguments suggest that the domain boundaries should not produce steps.[14] In a theoretical study by Roelofs *et al.*,[21] on the other hand, the deconstruction transition was investigated by the extended embedded-atom method (EAM), and the activation energy for a monoatomic step in the [001] direction was found to be very low and of the same order as the activation energy for a domain wall, which suggests that steps play an important role in initiating ordering. Therefore, the authors concluded that "the calculated static energies that emerge from this approach support the hypothesis that steps are involved in the genesis of order in the missing

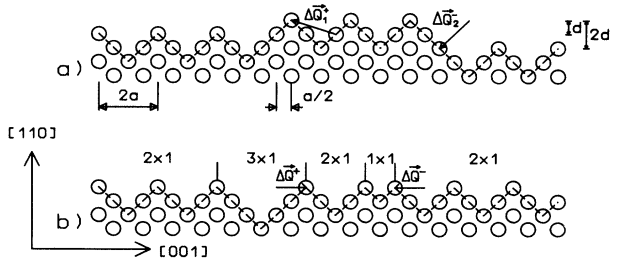

FIG. 1. Cross section of a (2×1)-reconstructed fcc(110) surface (a) with steps, and (b) with domain walls (Ising defects), but without steps. In (a), the displacement vectors $\Delta\mathbf{Q}_n^{\pm}$ for a monoatomic step-up and a double step-down and in (b), the displacement vectors $\Delta\mathbf{Q}_I^{\pm}$ according to each type of Ising defect considered, are shown as arrows.

row-type structures." Also the pronounced anisotropy of the step formation found by those authors is remarkable. Also other theoretical studies of reconstructed fcc(110) surfaces based on a modified solid-on-solid (SOS) model[16–18,20] independently predicted the existence of monoatomic steps already below T_c. As opposed to the KT roughening transition, this was termed preroughening.[20] This preroughening may be a precondition for step-induced deconstruction and the roughening transition for premelting. Molecular-dynamics calculations seem to show that the Au(110) surface starts to melt already below some 1000 K.[22]

This study was conducted to prove various theoretical predictions of roughening phenomena. The main questions were whether preroughening as predicted occurs at $T < T_c$, whether step formation influences the deconstruction transition, and whether the roughening transition occurs at $T \approx T_c$ (Ref. 15) or at $T = T_c + \Delta T$.[14,16,18] In Ref. 14, ΔT was predicted to be approximately 100 K. In the course of this investigation some new results related to the phenomena discussed above were published based on LEED,[23] x-ray diffraction,[24] thermal energy atom scattering (TEAS) with helium atoms,[25] and low-[12] as well as medium-[26] energy ion scattering.

LEED experiments[23] provided some first evidence of preroughening and a roughening transition at $T > T_c$. The temperature dependence of superlattice and integral-order peaks was observed in a synchrotron x-ray study[24] to study the deconstruction transition, and surface roughening was observed above T_c, with a difference of less than 50 K between the two transition temperatures. It was concluded from the temperature dependence of the width of the antiphase specular peak studied by TEAS (Ref. 25) that the Au(110) surface undergoes a roughening transition at about 40 K above T_c. Furthermore, it was shown that, above T_c, the diffraction profile changes from Lorentzian to power law as expected for a KT roughening transition. Low-energy ion-scattering experiments[12] demonstrated that the threshold for vacancy formation in the $[1\bar{1}0]$ strings is 120 K below T_c, while the threshold for the formation of atomic steps is around T_c. Recently, indications of surface roughening and evidence of surface premelting were found in medium-energy ion-scattering (MEIS) experiments.[26]

In this paper, results will be reported of high-resolution low-energy electron-diffraction (HRLEED) experiments for the temperature-dependent structure of the Au(110) surface in the range between room temperature and 786 K. The profiles of the specular (00), the half-order $(\frac{1}{2}0)$, $(\frac{\bar{1}}{2}0)$, and the fundamental (10), $(\bar{1}0)$ Bragg peaks were measured in a wide energy range between 16 and 164 eV at temperatures between 298 and 643 K and between 16 and 73 eV at higher temperatures. The step density was derived from the FWHM of the (00) peak and the shift of the half-order peak positions as a function of perpendicular momentum transfer $k_\perp$, which leads to an average terrace-width and step-height distribution. In measurements of the FWHM of the (00) peak in the two main crystallographic surface directions ([001] and $[1\bar{1}0]$), a strong asymmetry of the step density below T_c was observed, as had been proposed in the theoretical work of Roelofs *et al.*[21] Oscillations of the half-order peak position as a function of $k_\perp$ were detected by HRLEED for the first time. Just above T_c we detected a surface smoothing. At $T > 700$ K we determined steps with multiple-height steps, which indicate the beginning of the roughening transition.

Section II will contain a short description of the experimental conditions. The theoretical background of the data analysis is given in Sec. III; the results are described in Sec. IV and discussed in Sec. V.

II. EXPERIMENT

As has been shown in earlier studies of surface structures, HRLEED (Refs. 27–34) is well suited to surface-defects analyses. Details of the high-resolution low-energy electron diffractometer used in this study—the so-called SPA-LEED (spot-profile analysis LEED)—have been described previously.[27] In this type of diffractometer the diffraction angle between the incident and the outgoing electron beam is fixed at 7.5°.

The diffractometer is mounted to a vacuum chamber with a base pressure of $p = 5 \times 10^{-11}$ mbar and with the sample at room temperature. The commercial Au crystal was spark-cut as a disk (10 mm in diameter, 2 mm thick) from an Au ingot. The surface was aligned to the (110) plane within 0.17° and showed a mosaic spread of less than 0.17° averaged over the whole sample area as verified by x-ray diffraction.

The sample was mounted to a molybdenum holder by means of two thin Mo plates fitting into a notch (0.5 mm wide) on the circumference of the crystal. The sample holder was heated with a bifilar resistance heater. With this setup, temperatures up to 1200 K have been achieved. The temperature was measured with a NiCrNi thermocouple fixed at the edge of the crystal. For correct surface-temperature readings, the crystal was replaced by a polycrystalline gold dummy of the same size and shape. Another thermocouple was pressed onto the surface of that dummy and the temperature was calibrated with an accuracy of about 0.1 K. The temperature was controlled electronically and stabilized within ±1 K.

The polished crystal surface was prepared in a separate UHV chamber. The surface was cleaned with Ar^+ ions of 2 keV by successive sputtering (at room temperature) and annealing (at about 850 K) cycles. After several cycles, a diffuse (2×1) LEED pattern was observed. Additional sputtering and annealing cycles with 500-eV Ar^+ ions at 523 K produced a well-ordered (2×1) structure. The cleanness of the surface was checked by Auger-electron spectroscopy (AES). After this cleaning procedure no contamination was detectable on the surface, but after several hours of annealing at 800 K we observed approximately 0.07% of a Ca monolayer on the surface. To reduce this contamination the sample was heated to 800 K for several hours and afterwards sputtered again at 523 K. This procedure was repeated until the contamination had been reduced again below the detection limit of AES to allow experiments to be made without any surface contamination at 786 K for a period of more than 48 h.

During transfer to the SPA-LEED chamber the sample remained fixed to the Mo holder to avoid physical damage and stress. After its transfer in air it was possible to prepare the surface again within a few cycles of sputtering with 500 eV Ar^+ ions and subsequent annealing at 523 K until sharp LEED spots appeared. Before each measurement started, the crystal surface was sputtered for 1–3 min and annealed for at least 8 h at 523 K to ensure a clean and well-ordered surface.

The SPA-LEED system has a momentum resolution parallel to the surface which corresponds to a spot width of 3.7×10^{-3} Å^{-1}.[27,32] In this study, however, the narrowest spots with a width corresponding to 2×10^{-2} Å^{-1} were observed at the in-phase energy of 72 eV. This enlarged peak width is mainly caused by crystal imperfections, such as the finite size of grains and the mosaic spread. Before a measurement was started, the crystal was kept at the selected temperature for 8–12 h to reach thermal equilibrium.

III. THEORETICAL

To analyze the experimental results we performed calculations with a one-dimensional model according to the kinematic-scattering theory developed by Lu, Lagally, and co-workers.[35–38] That model starts with a surface containing only randomly distributed and noninteracting steps (Markovian disorder[39,40]) and leads to the following geometrical terrace-width distribution:

$$P(W)=\gamma(1-\gamma)^{W-1} . \tag{1}$$

In this formula, γ is the probability of finding a step between sites $(W-1)$ and W. Therefore, $(1-\gamma)^{W-1}$ is the probability of finding no step when crossing $(W-1)$ lattice sites. In other words, $P(W)$ defines the probability of occurrence of terraces with a width of Wa, where a is the lattice constant in the direction considered. The average terrace width, $\langle W\rangle a$, is defined by

$$\langle W\rangle a = a\sum_W WP(W) . \tag{2}$$

In Ref. 37 the average terrace width for a Au(110) surface was defined as $(\langle W\rangle-1)a$ and for the geometric terrace-width distribution given in Eq. (1), this average terrace width can be calculated by[37]

$$(\langle W\rangle-1)a=\left[\frac{1-\gamma}{\gamma}\right]a . \tag{3}$$

For the (2×1) surface the lattice constant in the [001] direction is doubled, compared to the (1×1) structure [for Au(1×1): $a=4.08$ Å at $T=300$ K].

To calculate an intensity profile by means of a geometric terrace-width distribution, a complex "boundary structure factor" is introduced according to[37]

$$f=1-\gamma+\gamma\{\beta e^{i[(a-2)k_\parallel a+k_\perp d]}+(1-\beta)e^{i[(\alpha-2)k_\parallel a-k_\perp d]}\} \equiv\rho e^{i\Psi} , \tag{4}$$

which describes an average phase factor associated with neighboring lattice sites along the reconstructed [001] direction, with only monoatomic step heights on the surface. $k_\parallel$ and $k_\perp$ are the parallel and perpendicular components, respectively, of the momentum transfer. β describes a step asymmetry ($\beta=1.0$ means a monotonic "step-up" case, and $\beta=0.5$ means no misorientation, i.e., equal probability for up and down steps), and d is the step height for a monoatomic step. The parameter α describes the phase shift of the surface lattice in the [001] direction due to a step on surfaces with $ABAB$ stacking. In our calculations, we assumed a commensurable phase shift which leads to a value of $\alpha=0.5$. The peak profiles can be calculated[35] in connection with Eq. (4) by the expression

$$I(k_\parallel a)=\frac{1-\rho^2}{1+\rho^2-2\rho\cos(2k_\parallel a+\Psi)} . \tag{5}$$

The peak profile $I(k_\parallel a)$ approximately corresponds to a Lorentzian. Among other things, from this relation it follows that the position of the half-order peaks will oscillate as a function of $k_\perp$,[37] an effect which has been observed in recent x-ray experiments on the Pt(110)(2×1) surface.[10] The analysis of diffraction data by comparing results according to Eq. (5) with experimental data reveals the density of monoatomic steps.

To also simulate models not restricted to the monoatomic step case, the boundary structure factor for monoatomic steps as given, Eq. (4) was expanded to the multilevel step case[35]

$$f=1-\gamma+\sum_{h=1}^{H}\gamma_h[\beta e^{i\Phi_h^+}+(1-\beta)e^{i\Phi_h^-}] , \tag{6}$$

where $\Phi_h^\pm$ is defined as the phase jump due to a step, "+" defines the "step-up" case, "−" the "step-down" case with $\Phi_h^\pm=\Delta\mathbf{Q}_h^\pm\cdot\mathbf{K}$, and $\Delta\mathbf{Q}_h^\pm$ is the shift of the lateral surface periodicity due to a step [see Fig. 1(a)] and $\mathbf{K}$ the total momentum transfer. Therefore, the phase jump can be written as

$$\Phi_h^\pm\equiv[(\alpha h-2)k_\parallel a\pm hdk_\perp] . \tag{7}$$

The values of γ_h are the probabilities for steps with height hd, satisfying the equation

$$\sum_{h=1}^{H}\gamma_h\equiv\gamma , \tag{8}$$

with H as the maximum step height in atomic units, d. For the reconstructed Au(110)(2×1) surface, domain walls have to be included in the boundary structure factor. These domain walls, like local (1×1),(3×1),... structures which produce no steps [see Fig. 1(b)], will be referred to below as "Ising defects." We considered only two different types of such defects, which produce the same phase shift, but with opposite signs

$$\Phi_I^\pm\equiv[\pm k_\parallel a] . \tag{9}$$

Φ_I^+ is the phase shift according to a (3×1) groove, and Φ_I^- is the shift due to a local (1×1) wall [Fig. 1(b)]. The "overall boundary structure factor" therefore can be

written as

$$f=1-\gamma-\epsilon+\sum_{h=1}^{H}\gamma_h\beta e^{i[(\alpha h-2)k_\parallel a+hdk_\perp]}+\sum_{h=1}^{H}\gamma_h(1-\beta)e^{i[(\alpha h-2)k_\parallel a-hdk_\perp]}+\epsilon[\lambda e^{-ik_\parallel a}+(1-\lambda)e^{ik_\parallel a}]\equiv\rho e^{i\Psi}. \quad (10)$$

In the last term, ϵ is the probability of finding an Ising defect and λ is an asymmetry term for the Ising defects [$\lambda=0.5$ means equal probability of (1×1) and (3×1) walls, and $\lambda=1.0$ allows only (1×1) walls]. The first term, $1-\gamma-\epsilon$, in Eq. (10) is the probability of finding neither steps nor Ising defects when going from one atomic position to the next. Obviously, γ and ϵ must satisfy the relation, $\gamma+\epsilon\leq1$.

We were able to confirm by calculations with different values of ϵ, that only the FWHM of the half-order peaks is influenced by the Ising defects. Also no significant change in all peak positions (half-order and integral-order) and in the FWHM of the (00) peak was found while varying ϵ. As a rough estimate we set $\epsilon=0.01$ in all calculations concerning the peak positions and FWHM of the (00) peak by applying Eqs. (5) and (10).

For simulation of the peak profiles above T_c, Eq. (10) was modified to allow a (1×1) structure to be described. In that case, "2" in the exponents must be replaced by "1." If we do not assume any interaction to take place between steps in the [001] and [1$\bar{1}$0] directions, this random-step model is also able to simulate the peak profiles in the [1$\bar{1}$0] azimuth.

Above the roughening transition temperature T_R, multiple steps are created and the peak profile should change from an approximate Lorentzian form [Eq. (5)] to a power law[30,41] expressed as

$$I(k_\parallel)=A\,|k_\parallel-g_{hk}|^{-[2-n(T)]},\quad A=\text{const} \quad (11)$$

with the magnitude of the reciprocal-lattice vector g_{hk}. The exponent $n(T)$ is a measure of the height-height correlation function in the case of a KT roughening transition and is a monotonically increasing function with rising temperature, as shown in a previous paper on the Pb(110) surface.[30] In particular, in the case of $T=T_R$ we have $n(T)=1$.

IV. RESULTS

A. General

With the diffraction angle of 7.5°, the relation between the momentum transfer $\mathbf{K}$ (in Å^{-1}) and E (in eV) is given by $|\mathbf{K}|=|\mathbf{k}_0-\mathbf{k}_i|=4\pi\cos(7.5°/2)(E/150.4)^{1/2}$. Thus, the perpendicular momentum transfer $k_\perp$ is defined by

$$k_\perp=\begin{cases}|\mathbf{K}| & \text{for the (00) peak}\\ [|\mathbf{K}|^2-(\pi/a)^2]^{1/2} & \text{for the } (\frac{1}{2}0) \text{ and } (\bar{\frac{1}{2}}0) \text{ peaks}\\ [|\mathbf{K}|^2-(2\pi/a)^2]^{1/2} & \text{for the (10) and } (\bar{1}0) \text{ peaks}.\end{cases} \quad (12)$$

In this study, the peak profiles, i.e., the intensity as a function of parallel momentum transfer $k_\parallel$ of the (00), $(\frac{1}{2}0)$, $(\bar{\frac{1}{2}}0)$, (10), and $(\bar{1}0)$ reflexes were measured at energies between 16 and 164 eV. These measurements were performed by variations of the deflection voltage applied to octopole field plates. To determine the peak position of the half-order and integral-order peaks in units of $k_\parallel$, the differences between the corresponding deflection voltages and the deflection voltage attributed to the (00) peak maximum were plotted as a function of E. The deflection voltage showed a square-root dependence, as expected.[42]

These measurements were done between 298 and 786 K. At temperatures above 643 K, the intensity of all spots decreased to the background level for energies higher than 72 eV. This is caused by the Debye-Waller factor [bulk Debye temperature of Au: $\Theta_{\text{Debye}}=174$ K (Ref. 43)] and the increased background. For all energies and temperatures the peaks showed no splitting or shoulders. This observation indicates a random distribution of steps (see Fig. 2).

The step density on the surface can be determined from the peak broadening and the shift of the half-order peak position as a function of $k_\perp$ as described in Sec. III. If the path difference of the electrons scattered from terraces with different height levels is a multiple of the electron wavelength, the electrons interfere in-phase, i.e., the perpendicular momentum transfer $k_\perp$ matches integer multiples of the reciprocal step height, $n2\pi/d$ or, in absolute units, $k_\perp\cdot d=n2\pi$, with $n=1,2\ldots$. The scatter-

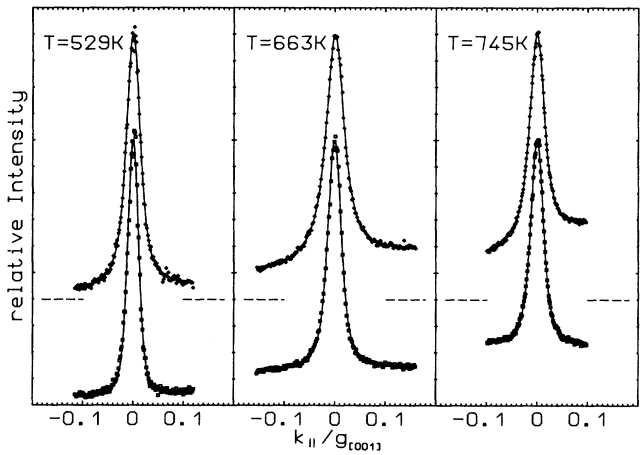

FIG. 2. Profiles of the (00) peaks at $k_\perp d=3\pi$ for three different temperatures. The maxima are normalized. The upper curves correspond to the [001] direction, the lower ones, to the [1$\bar{1}$0] direction. The zero level of the upper curves is indicated by dashed lines. The solid curves are fits to the data. The fits are calculated according to Eq. (5) with parameters given in Table I and convoluted with the corresponding resolution function; furthermore, a linear background, as deduced from the raw data, was added after the convolution. The magnitude of the reciprocal-lattice vector $g_{[001]}$ is defined by $2\pi/a$ ($a=4.08$ Å). At this antiphase condition, the FWHM of the Gaussian contribution obeys a value of about half the width of the measured peak in the [001] direction at 529 K.

ing at $k_\perp \cdot d = (2n+1)\pi$, with $n = 0, 1, 2, \ldots$, is called an antiphase condition. It is known that the first interlayer spacings of the Au(110)(2×1) surface are relaxed.[7,8] Our results show that the step heights are always multiples of the bulk interlayer spacings d within a relative error of $<5\%$. For room temperature with $d = 1.44$ Å the following in-phase energies of the (00) peak were derived: $E = 18.2$ eV ($n = 1$), $E = 72.8$ eV ($n = 2$), and $E = 163.8$ eV ($n = 3$).

The measured peak profiles $I(k_\parallel)$ can be described by three different components: first, a Lorentzian function containing all information about steps on the surface; second, a Gaussian function including the instrumental resolution and crystal imperfections;[27,32] and third, an approximately linear background caused by diffuse scattering. All three components of the measured peak are energy dependent. Each measured profile was fitted to a functional form resulting from the convolution of the Lorentzian with the Gaussian and the additive linear background. This analysis was performed by this numerical procedure.

The width of the Gaussian was varied in discrete steps from zero (δ function) to the full width of the measured peak. For each Gaussian, the parameters of the Lorentzian and the linear background were varied until a minimum in χ^2 was found. Fitting a polynomial to χ^2 as a function of the Gaussian widths, we determined the optimal Gaussian FWHM by looking for the absolute minimum in χ^2. This yields the FWHM of the Lorentzian, but with a large error at the in-phase energies. Therefore, a different analysis was applied to the Lorentzian FWHM. The energy-dependent Gaussian widths resulting from the convolution fit, as described above, were smoothed with splines (e.g., solid line in Fig. 3). All those curves did not show any significant dependence on the sample temperature. The values of the smoothed curves were used to calculate the Lorentzian FWHM with the empirical formula,

$$l = x - \frac{g^2}{x} . \tag{13}$$

In this expression, x is the FWHM of the measured peak, g the FWHM of the Gaussian resolution function, and l of the Lorentzian peak profile [Eq. (5)]. The FWHM x of the measured peak was determined from the raw data by a numerical procedure in which the background was assumed to be linear under the peak. We found the empirical formula Eq. (13) by numerical analysis of convolutions of Lorentzian with Gaussian peaks. This formula was seen to be correct within a relative error on the order of 10^{-7}.[42] The Lorentzian FWHM calculated in this way is in excellent agreement with the results of the convolution fits at the antiphase energies.

B. Peak shifts

In an earlier paper, Robinson found a peak shift of the half-order peak on the Au(110)(2×1) surface at 300 K.[5] A more detailed x-ray study of the Pt(110)(2×1) (Ref. 10) surface by Robinson, Vlieg, and Kern revealed a temperature-dependent oscillatory peak shift as a function of $k_\perp$. The oscillatory peak shifts could be attributed to steps, as proposed in a theoretical study by Fenter and Lu[37] according to their theoretical description discussed above [Eqs. (4) and (5)]. The amplitude of the oscillation is a direct measure of the average terrace width

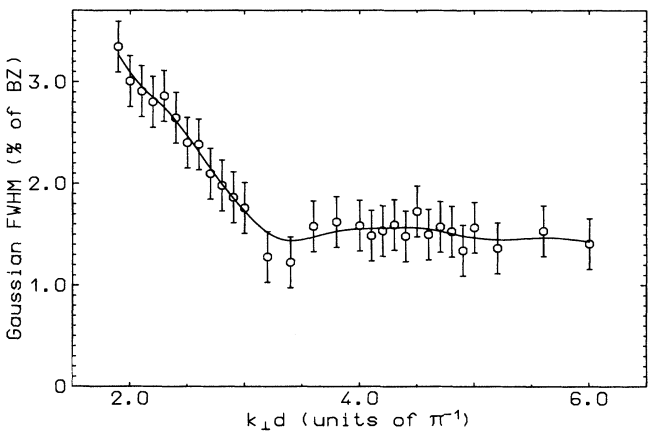

FIG. 3. Width of the Gaussian at $T = 529$ K as a function of $k_\perp$. The points are the results of the procedure of fitting (see text) to the (00) peak in the [001] direction. The solid curve is a smoothing spline fit used for the deconvolution of the measured FWHM according to Eq. (13). The error bars indicate the step width of the Gaussian FWHM of the fitting procedure.

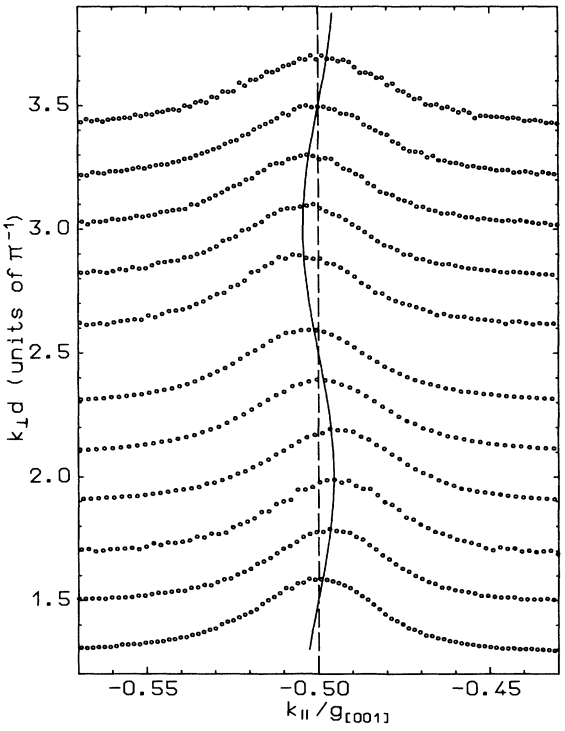

FIG. 4. Spot profiles of the $(\frac{1}{2}0)$ peak for different $k_\perp$ at $T = 663$ K. Each profile is normalized to its maximum. The maximum of each peak indicates the corresponding $k_\perp$. The solid curve is the result of a model calculation according to Eqs. (4) and (5). The parameters of this calculation were $\alpha = 0.5$, $\gamma = 0.043$, and a step asymmetry of $\beta = 0.314$, which leads to a misorientation angle $\Theta = -0.17°$.

$(\langle W\rangle-1)a$. In HRLEED experiments, similar oscillations were found by He, Zuo, and Wang[33] at the edge of a Pt(110)(2×1) crystal at room temperature, where additional steps and a misorientation due to a rounding effect during polishing occurred. Furthermore, He, Zuo, and Wang found an oscillation of the (00) peak position which was attributed to the misorientation of the surface with respect to the (110) plane. Such behavior was predicted in a theoretical study by Presicci and Lu.[36]

Figure 4 shows the measured $(\frac{1}{2}0)$ peak profiles as a function of perpendicular momentum transfer as measured by SPA-LEED on the Au(110)(2×1) surface. This result yields an obvious oscillatory shift of the peak maxima. No additional structures appear in the peak profiles. Figure 5 shows the $k_\perp$ dependence of the positions of all measured nonspecular peaks at 298 K. The oscillations were detected over two periods, corresponding to an energy range from 16 to 164 eV, for temperatures up to 642 K. Using Eqs. (5) and (10) we calculated the peak positions as a function of $k_\perp$ for different sets of parameters and compared them to the oscillations presented in Fig. 5. All peak positions were determined numerically from Eq. (5) within a relative accuracy of 10^{-5}. By comparing the measured data with the calculated ones, shown in Fig. 5 as solid lines, we found the parameters, $\gamma=0.030$, $\beta=0.209$ for Figs. 5(a) and 5(b), and $\gamma=0.047$, $\beta=0.320$ for Figs. 5(c) and 5(d) as best fits to the data. Both values of β yield a mean misorientation of $\Theta=-0.17°\pm0.02°$ of the surface with respect to the (110) plane projected on the [001] direction, calculated from the following expression,[37] with $\alpha=0.5$:

$$\Theta=\arctan\left[\frac{(2\beta-1)\gamma d}{(2+\alpha\gamma)a}\right]. \tag{14}$$

The value derived for Θ corresponds to the error in surface orientation (see Sec. II) due to the cutting of the crystal.

The different oscillation amplitude of equivalent positions of peaks, e.g., (10) and $(\bar{1}0)$, is due to an asymmetry of the SPA-LEED optics and has been taken as an estimate of the maximum errors shown as bars in Fig. 5. No change in the misorientation angle Θ of the surface was observable for temperatures between 298 and 786 K within the error of $\Delta\Theta=0.02°$.

In Fig. 6(a) we present the temperature dependence of the amplitude of the shift for the half-order peaks. The

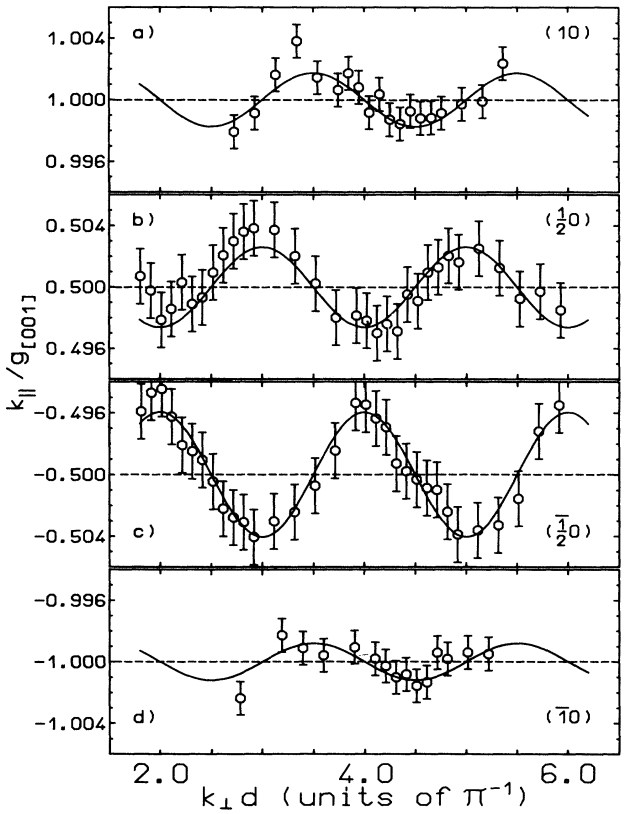

FIG. 5. Positions of the peak maxima as a function of $k_\perp d$ for nonspecular peaks at $T=298$ K measured in the [001] direction: (a) (10) peak, (b) $(\frac{1}{2}0)$ peak, (c) $(\frac{\bar{1}}{2}0)$ peak, and (d) $(\bar{1}0)$ peak. The error bars indicate an estimated error due to the asymmetric oscillations of the $(\bar{n}0)$ and the $(n0)$ peak positions. The solid curves are results of fits using Eqs. (4) and (5) with the parameters given in the text.

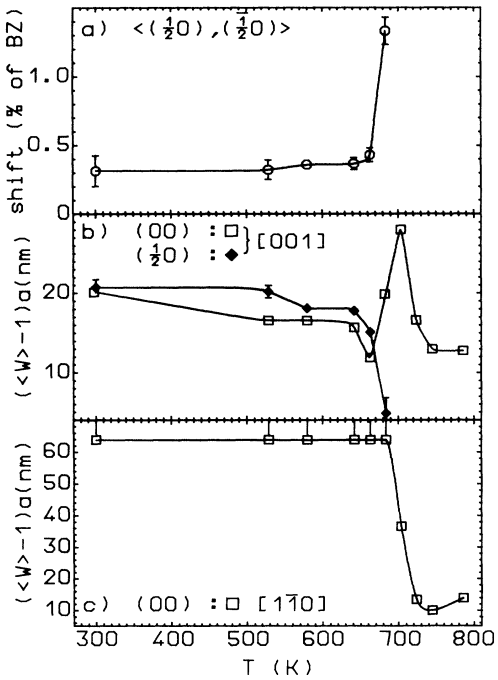

FIG. 6. Peak shift and average terrace width as a function of temperature. (a) The amplitude of the peak-shift oscillations averaged for the $(\frac{1}{2}0)$ and the $(\frac{\bar{1}}{2}0)$ peaks, (b) the average terrace width $(\langle W\rangle-1)\,a$ for the [001] direction as determined by the γ values given in Table I (open squares) and by the amplitude of the peak-shift oscillations of the half-order peaks (solid diamonds), (c) the average terrace width $(\langle W\rangle-1)a$ for the $[1\bar{1}0]$ direction as determined by the γ values given in Table I. The vertical lines at the points between 298 and 683 K indicate that the points are only lower limits of the terrace size. The other curves are spline fits to the data designed to guide the eyes.

shift is determined by fits to the measured oscillations for each temperature, as shown in Fig. 5 for $T=298$ K. There is a slight increase in the amplitude from room temperature up to 642 K. Above 642 K a stronger increase in the shift is seen. In Fig. 6(b) the solid diamonds denote the average terrace width deduced from Eq. (3) with the γ values for each temperature which result from the fits to the oscillations of the peak positions. A detailed discussion of this fact can be found in Sec. V of this paper.

C. FWHM of the integral-order peaks

From the measured profiles of the (00) peak the deconvoluted FWHM were determined as a function of $k_\perp d$ for each temperature by the procedure described above [Eq. (13)]. The results are shown in Fig. 7 for the [001] (a) and $[1\bar{1}0]$ (b) directions. These results are compared to model calculations. The best fits are shown as solid lines for each temperature and the corresponding fit parameters are presented in Table I.

Let us concentrate first on the shape of the FWHM oscillations. For the [001] direction at $T=298$ K we see an oscillation which is due to monoatomic steps and a small amount of double steps ($\approx 10\%$) as revealed by model calculations. At higher temperatures up to 704 K, only monoatomic steps are present within a detection limit for higher steps of less than 5%. For the $[1\bar{1}0]$ direction, no oscillations are detectable for temperatures up to 684 K. The relatively large fluctuation of the FWHM values at 298 K for the $[1\bar{1}0]$ direction is due to the deconvolution procedure and can be used to estimate the maximum error of this procedure (see comment in Ref. 44). No oscillations are detectable below about 680 K. Above 704 K, clear oscillations appear for both directions, but the shape of the oscillations is different from the shape at lower temperatures in the [001] direction. These different shapes can be attributed to multilevel steps as shown by the detailed analysis (see Table I) and the discussion below.

There is a strong anisotropy in the step density below 704 K for the [001] and $[1\bar{1}0]$ directions. This result corroborates the result of model calculations by Roelofs *et al.*[21] The widths for the $[1\bar{1}0]$ directions show no oscillations, as is evident from Fig. 7(b) for $T=298$ K and, therefore, the missing-row structure must extend over more than 640 Å in the $[1\bar{1}0]$ direction. From the comparison of the experimental data with calculated data we obtained the average terrace widths corresponding to the γ values (Table I) as a function of the temperature of both main crystallographic symmetry directions ([001] and $[1\bar{1}0]$). The results are shown in Figs. 6(b) and 6(c). For all temperatures above 684 K, the change of the unit cell in the [001] direction was considered for the calculations. If we compare the average terrace width determined by the peak shift of the half-order peak [solid diamonds in Fig. 6(b)] with the terrace width obtained from the FWHM of the (00) peak [open squares in Fig. 6(b)], the two terrace widths are similar below T_c, but differ significantly at 684 K. We shall discuss this discrepancy in Sec. V B.

In Fig. 8 the deconvoluted FWHM of the (00), (10),

TABLE I. Parameters resulting from best fits to the FWHM oscillations are presented in Fig. 5. For all calculations we used $\alpha=0.5$, and assumed a misorientation angle of $\Theta=-0.17°$. The step probability γ is defined in Eq. (1). The columns with $h=1,\ldots,$ show the probabilities γ_h for each individual step height [see Eq. (8)]. The last column contains the average step height $\langle H\rangle$. The horizontal line between 684 and 704 K indicates the change from the (2×1) structure to the (1×1) structure. All values are within an estimated error of approximately $\pm5\%$.

T (K)	γ	$h=1$	$h=2$	$h=3$	$h=4$	$h=5$	$\langle H\rangle$
			[001] direction				
298	0.039	90%	10%				1.1
529	0.047	100%					1.0
580	0.047	100%					1.0
642	0.050	100%					1.0
663	0.064	100%					1.0
684	0.040	100%					1.0
704	0.014	100%					1.0
725	0.024	83%	7%	4%	6%		1.3
745	0.031	70%	13%	9%	8%		1.6
786	0.031	58%		15%	18%	9%	2.2
			$[1\bar{1}0]$ direction				
298	<0.004						
⋮	⋮						
684	<0.005						
704	0.008	100%					1.0
725	0.021	72%	6%	11%	11%		1.6
745	0.028	57%	10%	20%	9%	4%	1.9
786	0.020	68%	7%	13%	12%		1.7

and $(\frac{1}{2}0)$ peaks are presented as measured for different electron energies as a function of the temperature. The values for the (00) peaks shown in Figs. 8(b) and 8(c) were obtained from the widths of the calculated peak profiles under the antiphase condition ($k_\perp d = 3\pi$) with the parameters presented in Table I. The width of the (10) peak, which was also measured under an antiphase condition ($k_\perp d \approx 4\pi$), in principle shows a temperature dependence similar to that of the width of the specular reflex [Fig. 8(b)]. The FWHM of the half-order peak [Fig. 8(a)] is constant up to 642 K and shows a strong increase for higher temperatures, which indicates the decay of the order in the reconstructed domains. From the deconvoluted FWHM of the half-order peaks $(\frac{1}{2}0)$, a deconstruction temperature of $T_c = 654 \pm 10$ K was estimated by application of the equation for the critical behavior of the correlation length.[13] As the FWHM was measured only at two temperatures above T_c, as shown in Fig. 8(a), the error for T_c is relatively large. This deconstruction temperature T_c is between two extremely different values as indicated in the literature [$T_c = 545$ K (Ref. 45) and $T_c = 735$ K (Ref. 24)]. This difference in T_c may be attributed to traces of impurities on the surface and/or to the influence of finite-size effects.[45] Additionally, as mentioned by Keane *et al.*,[24] it can be related to different resolutions of the diffraction methods used.

The FWHM of the specular peak in the [001] direction shows a very interesting temperature dependence [see Figs. 8(b) and 8(c)]. First, we see a slight increase below T_c. Around T_c, the width increases more rapidly, indicating the enhanced creation of monoatomic steps around the deconstruction transition. But above 663 K, the FWHM falls below the value at room temperature. The smallest width is observed at 704 K. This unexpected behavior gives rise to the assumption that the surface becomes smoother above the deconstruction transition. Above 704 K, however, the width increased again and the evolution of multiple-height steps was observed, indicating the onset of the roughening transition. An estimate of the roughening temperature of $T_R = 710 \pm 10$ K is given. The estimated roughening temperature is in agreement with a result of a recent experiment with thermal helium-atom scattering (TEAS).[25] As seen in Table I, the

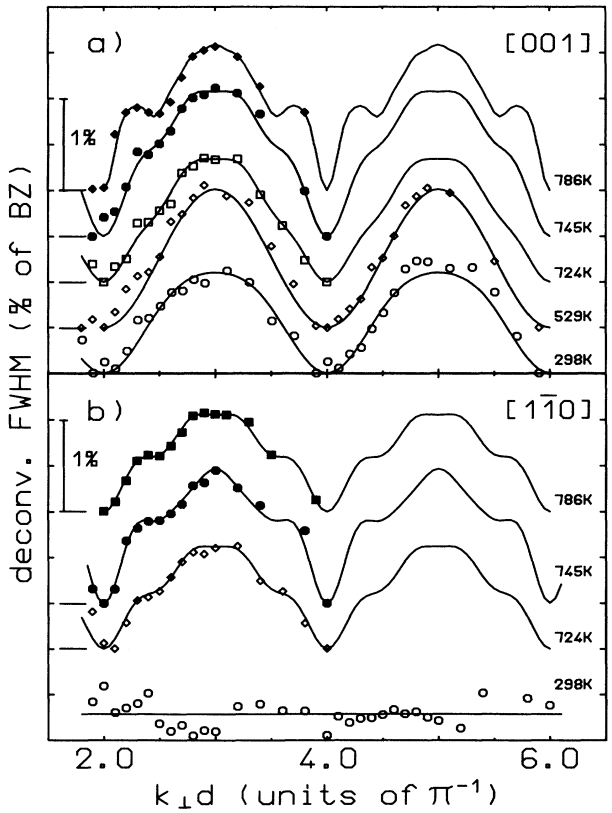

FIG. 7. FWHM of the deconvoluted (00) peak as a function of $k_\perp d$ for various temperatures in the (a) [001] and (b) [1$\bar{1}$0] directions. The oscillations are shifted with respect to each other for clearer representation. No significant changes in shape can be observed between 529 and 704 K (a) and between 298 and 704 K (b). The solid curves are best fits to the data according to Eqs. (4) and (5) with the parameters given in Table I. The statistical errors are smaller than the symbol size. The relatively large scattering of the data points at $T = 298$ K in (b) is due to the fitting procedure (see the comment in Ref. 44). The solid line is a linear fit to the data. Zero FWHM is indicated by a short line on the abscissa for each dataset.

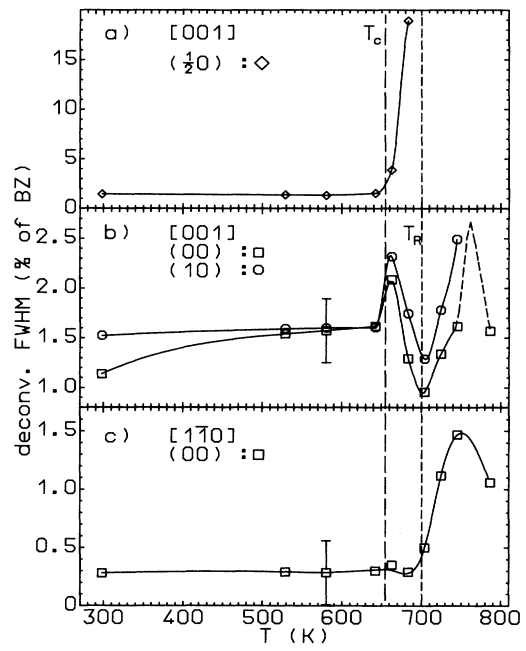

FIG. 8. Deconvoluted FWHM as a function of temperature for various peaks and directions. (a) $(\frac{1}{2}0)$ reflex at $E = 32.8$ eV ($k_\perp d = 2.66\pi$) in [001]; (b) (00) reflex at $E = 40.5$ eV ($k_\perp d = 3\pi$) and (10) reflex at $E = 72.0$ eV ($k_\perp d = 3.94\pi$), both in [001]; (c) (00) reflex at $E = 40.5$ eV ($k_\perp d = 3\pi$) in the [1$\bar{1}$0] direction. All solid curves represent spline fits to the data designed to guide the eyes. The dashed line in (b) connecting the two high-temperature points indicates that the FWHM of the (00) spot has its maximum at about 765 K. This was found by repeated measurements with standard LEED (Ref. 23). The dashed vertical lines indicate the locations of T_c and T_R in this study.

average step height increases, as expected for roughening. The temperature dependence of the FWHM for the (00) peak will be discussed in the next section on the basis of a simple model.

As expected for a KT-type roughening transition, the peak profile should change from Lorentzian [Eq. (5)] to a power law [Eq. (11)].[30,41] In contrast to recent TEAS results[25] on the Au(110) surface, we found no significant change in the deconvoluted peak profile. A change from a Lorentzian to a power law is expected when the temperature changes from $T < T_R$ to a temperature $T > T_R$ (see the solid line in Fig. 2, where Lorentzians convoluted with Gaussian functions fit the data well, even for $T > T_R$).

V. DISCUSSION

Let us now discuss a structural model and so describe the temperature dependence of the experimental results. Let us consider five different temperature ranges in connection with different phases for the structure on the Au(110) surface.

(1) The low-temperature (2×1) reconstructed phase $(T \ll T_c)$.

(2) The $(2\times1)\leftrightarrow(1\times1)$ mixed-phase $[(T_c-\Delta T < T < T_c+\Delta T)$ range of deconstruction transition].

(3) The smooth (1×1) phase above T_c $(T_c < T < T_R)$.

(4) The rough phase above T_R $(T_R < T < T^*)$.

(5) The smoothed, laterally disordered quasiliquid phase $(T > T^*)$.

A. The low-temperature (2×1) reconstructed phase $(T \ll T_c)$

In the low-temperature range no completely flat surface is found in the [001] direction, as reported already by other authors.[1,4,5,24,25] Reasons for the appearance of monoatomic steps parallel to the $[1\bar{1}0]$ direction are given by Roelofs *et al.*[21] For the $[1\bar{1}0]$ direction, the missing-row structure extends at least over more than 640 Å subject to the limit of resolution of the instrument. At room temperature we find a small number of double steps in the [001] direction which disappear above 529 K. This might be due to additional annealing. Before the measurement at $T=298$ K started, the crystal had been annealed for 24 h at 529 K. After the measurement at $T=298$ K the temperature had been raised again to 529 K and maintained for more than 48 h before the measurement at 529 K started. Therefore, we conclude that annealing for more than 72 h at 529 K is needed to remove thermodynamically unstable double steps and that in equilibrium at $T < T_c$ only monoatomic steps parallel to the $[1\bar{1}0]$ direction would appear.

Qualitatively, such behavior corresponds to the preroughening phenomenon predicted by den Nijs[20] and other authors.[16–18] These theoretical studies revealed that a preroughened state may exist on unreconstructed fcc(110) surfaces below the temperature of the KT-type roughening transition which is characterized by the presence of monoatomic steps only. Unlike the predictions, these experiments have shown that preroughening appears also on a reconstructed fcc(110) surface.

Steps in the [001] direction were observed whereas, in the $[1\bar{1}0]$ direction, no steps develop [Figs. 8(b) and 8(c)]. From this result we would conclude that the surface is in a preroughened state, as proposed by den Nijs[20] and other theoretical studies.[16–18] The anisotropy observed is in agreement with the theoretical description by Roelofs *et al.*[21]

B. The $(2\times1)\leftrightarrow(1\times1)$ mixed phase $[(T_c-\Delta T < T < T_c+\Delta T)$, range of deconstruction transition]

The temperature range in which the deconstruction transition takes place and different structures coexist is indicated by ΔT. The role of steps in this transition is an essential feature to be clarified by experiments since first theoretical models have been worked out.[14–18,20,21]

In the range between T_c-10 K and T_c+10 K, a significant enhancement of the step density can be detected. This effect is reproduced by the peak shift of the half-order peak [Figs. 6(a) and 6(b)] and by the FWHM of the (00) and (10) peaks under the antiphase conditions [Fig. 8(b), $k_\perp d = 3\pi(00)$ and $k_\perp d \approx 4\pi(10)$, respectively]. In the $[1\bar{1}0]$ direction no change of the FWHM of the (00) peak is observed so that the increase in step density at the deconstruction transition is assumed to occur only in the [001] direction.

At 684 K there is a discrepancy in the average terrace widths resulting from the $(\frac{1}{2}0)$ peak shift and from the width of the specular reflex (see Fig. 6). While the calculation of the average terrace width from the peak shifts furnishes a relatively small average terrace width of about 5 nm, the width calculated from the FWHM of the (00) spot is about 20 nm. This observation is explained as follows.

At temperatures around T_c, domains with different surface structures coexist, e.g., as proposed by model calculations.[18] The peak shift of the half-order peak is only sensitive to domains on the surface where a (2×1) structure exists. However, the FWHM of the (00) peak is determined by (2×1) as well as by (1×1) domains. If the height levels for two different (2×1) domains, which are separated by a (1×1) domain, differ by one unit d, a correspondingly large shift of the $(\frac{1}{2}0)$ peak is caused. This situation is visualized in Fig. 9(a), where two (2×1) domains with widths $W1$ and $W2$ are separated by the distance, $D \gg W1+W2$. If D is less than the transfer width, electrons diffracted from both (2×1) domains will interfere with each other. As both domains are at a different height level, the half-order peak position is determined by the step between the two domains. Therefore, the average terrace width calculated from the peak shift is $(W1+W2)/2$. The specular reflex, on the other hand, does not distinguish between reconstructed and (1×1) domains. Thus, the average terrace width deduced from the FWHM of the (00) profile is $(W1+D+W2)/2$, which is larger indeed. The terrace width, averaged over the surface area covered by the electron beam and containing (2×1) and (1×1) domains, appears to be larger, i.e., the surface appears to be smoother, when derived from the (00) peak FWHM rath-

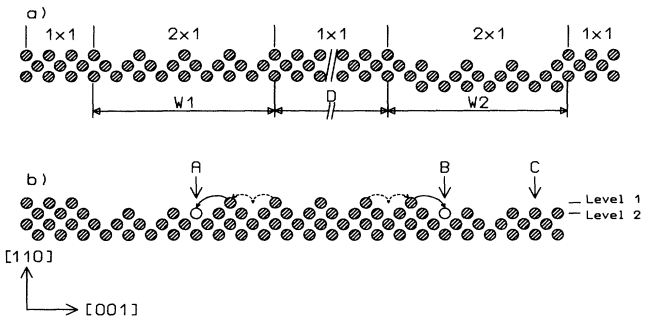

FIG. 9. Cross section of the Au(110) surface at $T_c < T \ll T_R$. (a) Mixed phase with steps, (b) stepped (2×1) surface illustrating the mechanism of smoothing above T_c. For details, see text.

er than from the $(\frac{1}{2}0)$ peak position.

For calculation of the average terrace width at 684 K by Eq. (3), a (2×1) surface was assumed. However, near T_c the surface contains (2×1) and (1×1) domains, as expected for a second-order phase transition[19] and, hence, the question arises whether the calculated average terrace width therefore depends on the size of the unit cell in the [001] direction. When a change is made to a model surface in the pure (1×1) state, the resulting γ will change by a factor of about 2. This will be compensated by the change in the lattice parameter a by a factor of $\frac{1}{2}$. Therefore, the average terrace width for small γ calculated for the (1×1) structure from Eq. (3) is approximately the same as that for a (2×1) structure. This approximation was checked numerically. The expected difference in terrace widths as presented in Figs. 6(b) and 6(c) is smaller than the size of the symbols.

C. The smooth (1×1) phase above T_c ($T_c < T < T_R$)

We assumed that deconstruction into the (1×1) structure is complete at $T\approx704$ K because the half-order peaks were no longer seen. At that temperature, the surface is flatter, i.e., the terrace width in the [001] direction is larger by a factor of about 4, compared to the low-temperature range $T \ll T_c$. During deconstruction, there is considerable mass transport to form a (1×1) structure.

Figure 9(b) will help discussing the smoothing of the surface above T_c, based on the presence of steps on the surface near T_c. Surface atoms of the (1×1) structure (site *C*) are higher coordinated than those of the (2×1) structure and, therefore, will have a higher binding energy than atoms at top sites of the (2×1) structure. Because of steps on the surface, level 1 is not completely filled with atoms. Due to the migration of atoms in the outermost layer of the (2×1) domains the empty sites of level 2 (sites *A* and *B*) will successively be filled at the expense of the population of level 1. Therefore, steps are removed and a flat (1×1) structure is created. According to our results obtained at $T=704$ K, smoothing obviously, as is to be expected, is effective only in the [001] direction, as we observe a decrease by a factor of 2 in the average terrace width in the $[1\bar{1}0]$ direction.

D. The rough phase above T_R ($T_R < T < T^*$)

A roughening transition takes place at a temperature above 704 K. The measurements show an increased FWHM of the (00) peak in both surface directions resulting in a decreased average terrace width [see Fig. 6(b)]. In accordance with the theory of roughening,[46] the increase in average step height $\langle H \rangle$ is observed directly. The relative probabilities of each individual step height are given in Table I. A decrease of the relative probability of single-height steps, with increasing temperature and an increased probability of occurrence of higher steps up to fivefold steps, is evident. At $T=745$ and 786 K, the average terrace width has approximately the same value for both main symmetry directions. The slight difference in the results for the [001] and $[1\bar{1}0]$ directions does not exceed the uncertainties of the values.

Although a roughening transition had been detected in the analysis of the oscillations of the FWHM of the (00) peak, we did not observe an influence of this transition on the shape of the peak profiles themselves. In the case of the KT roughening transition, a change from a Lorentzian [Eq. (5)] to a power-law profile [Eq. (11)] would have been expected.[41] Therefore, two possible reasons for the experimental results will be discussed.

First, the roughening transition may not be of the KT type. van Beijeren and Nolden[46] discussed the possibility of roughening transitions not attributable to the KT class because the roughening transition is affected by impurities. In this case, undetectable traces of impurities of Ca or other elements could have caused the behavior observed. The second explanation lies in the relatively large Gaussian width at the $k_\perp$ values considered. The Kummer function, which is a power law convoluted with a Gaussian, cannot be distinguished clearly from a Lorentzian convoluted with a Gaussian, if the width of the Gaussian is large compared to peak broadening due to steps.

We believe the second explanation to be the most reasonable, for the increasing average step height with increasing temperature indicates the divergence of the height-height correlation, as expected for KT roughening.[46]

E. The smoothed, laterally disordered quasiliquid phase ($T > T^*$)

In a recent ion-scattering study[26] the Au(110) surface was shown to start melting at a temperature of $T^*=770$ K. This formation of a laterally disordered quasiliquid layer gives rise to the assumption that surface roughening is a precursor to the premelting observed. The steps created at $T > T_R$ disappear at temperatures above T^* because of the enhanced lateral diffusion. The enhanced diffusion in the quasiliquid state was detected on the Pb(110) surface.[47]

Our conclusion concerning smoothing of the surface above the roughening transition is confirmed in a recent study with standard LEED,[23] in which a decrease of the FWHM above 780 K was found to indicate smoothing of the surface. In those measurements, the FWHM of the (00) peak has its maximum at about 765 K. This is indi-

cated in Fig. 8 by the dashed line connecting the points at 745 K and 786 K as published previously.[23] It was possible to reproduce the decreasing FWHM by repeated measurements with standard LEED. In a study by Yang, Lu, and Wang, the Pb(111) surface[28] showed a similar smoothing behavior.

VI. CONCLUSIONS AND SUMMARY

We studied the structure of the Au(110) surface as a function of the temperature by HRLEED. Investigating the (00), $(\frac{1}{2}0)$, $(\frac{\bar{1}}{2}0)$, (10), and $(\bar{1}0)$ peaks, we found oscillations of the peak positions of the half-order and integer-order peaks. For the Au(110) surface temperature-dependent peak shifts of the half-order peaks were observed for the first time. They might be attributable to monoatomic steps in the [001] direction at $T<T_c$. The oscillation of the integer-order peaks could be attributed to a misorientation of the surface.

From the temperature dependence of the FWHM of the half-order peaks we deduced the deconstruction temperature, $T_c=654\pm10$ K. The roughening temperature is estimated to be $T_R=710\pm10$ K from the observation of multiple-height steps above 704 K, which is in accordance with the result of a TEAS experiment.[25]

The FWHM as a function of $k_\perp$ of the (00) peak was determined in the temperature range between 298 and 786 K. An investigation of the FWHM of the (00) peak and the shift of the half-order peak position revealed evidence of the existence of monoatomic steps below T_c, with strong anisotropy with respect to the main crystallographic directions. We conclude that the Au(110) surface shows preroughening[16,18,20] below T_c. But the monoatomic steps appear only in the [001] direction.

In our opinion, the description of the deconstruction transition in the 2D Ising model will not imply restrictions concerning the creation of monoatomic steps and, therefore, our results are not in contradiction with the theoretical model as proposed by Villain and Vilfan.[14] In conformity with a theoretical paper[21] published recently we conclude that the presence of monoatomic steps is important for the deconstruction mechanism. Therefore, step formation may be a precondition of deconstruction.

Above T_c, the surface smooths down, i.e., the step density in [001] direction reaches the smallest value at 704 K. The roughening transition takes place after the deconstruction is completed.

The roughening transition was detected by the observation of multiple-height steps at $T>705$ K for steps appearing in the [001] as well as in the $[1\bar{1}0]$ directions. The analysis yielded up to fivefold step heights at 786 K. However, no significant change from Lorentzian to power-law behavior of the peak shape can be observed above T_R.

Our results of the roughening transition are in agreement with other experimental results of Au(110) (Refs. 24 and 25) with respect to the difference, $(T_R-T_c)\approx50\pm10$ K.

In summary, anisotropic preroughening and isotropic roughening have been detected on the Au(110) surface below and above the $(2\times1)\rightarrow(1\times1)$ transition, respectively. The deconstruction is influenced by steps.

ACKNOWLEDGMENT

We would like to thank J. Sprösser for very stimulating discussions.

[1]H. Jagodzinski, W. Moritz, and D. Wolf, Surf. Sci. **77**, 233 (1978).
[2]W. Moritz and D. Wolf, Surf. Sci. **88**, L29 (1979).
[3]J. R. Noonan and H. L. Davis, J. Vac. Sci. Technol. **16**, 587 (1979).
[4]G. Binning, H. Rohrer, Ch. Gerber, and E. Weibel, Surf. Sci. **131**, L379 (1983).
[5]I. K. Robinson, Phys. Rev. Lett. **50**, 1145 (1983).
[6]I. K. Robinson, Y. Kuk, and L. C. Feldman, Phys. Rev. B **29**, 4762 (1984).
[7]W. Moritz and D. Wolf, Surf. Sci. **163**, L655 (1985).
[8]K.-M. Ho and K. P. Bohnen, Eur. Phys. Lett. **4**, 345 (1987).
[9]K.-M. Ho and K. P. Bohnen, Phys. Rev. Lett. **59**, 1833 (1987).
[10]I. K. Robinson, E. Vlieg, and K. Kern, Phys. Rev. Lett. **63**, 2578 (1989); reply to comment by I. Vilfan and J. Villain, *ibid.* **65**, 1831 (1990).
[11]E. Vlieg, I. K. Robinson, and K. Kern, Surf. Sci. **233**, 248 (1990).
[12]E. van de Riet, H. Derks, and W. Heiland, Surf. Sci. **234**, 53 (1990), and references therein.
[13]J. C. Campuzano, M. S. Foster, G. Jennings, and R. F. Willis, Phys. Rev. Lett. **54**, 2684 (1985); J. C. Campuzano, G. Jennings, and R. F. Willis, Surf. Sci. **162**, 484 (1985).
[14]J. Villain and I. Vilfan, Surf. Sci. **199**, 165 (1988); I. Vilfan and J. Villain, Phys. Rev. Lett. **65**, 1830 (1990).
[15]A. C. Levi and M. Touzani, Surf. Sci. **218**, 223 (1989).
[16]J. Kohanoff, G. Jug, and E. Tosatti, J. Phys. A **23**, 5625 (1990).
[17]K. L. Murphy and C. Rottman, Phys. Rev. B **42**, 680 (1990).
[18]G. Jug and E. Tosatti, Phys. Rev. B **42**, 969 (1990).
[19]M. E. Fisher and R. J. Burford, Phys. Rev. **156**, 583 (1967).
[20]M. den Nijs, Phys. Rev. Lett. **64**, 435 (1990); **66**, 907 (1991).
[21]L. D. Roelofs, S. M. Foiles, M. S. Daw, and M. I. Baskes, Surf. Sci. **234**, 63 (1990), and references therein.
[22]F. Ercolessi, S. Iarlori, O. Tomagnini, E. Tosatti, and X. J. Chen, Surf. Sci. **251/252**, 645 (1991).
[23]U. Romahn, H. Zimmermann, M. Nold, A. Hoss, H. Göbel, P. von Blanckenhagen, and W. Schommers, Surf. Sci. **251/252**, 656 (1991).
[24]D. T. Keane *et al.*, Surf. Sci. **250**, 8 (1991).
[25]J. Sprösser, B. Salanon, and J. Lapujoulade, Eur. Phys. Lett. **16**, 283 (1991).
[26]A. Hoss, M. Nold, P. von Blanckenhagen, and O. Meyer, Phys. Rev. B **45**, 8714 (1992).
[27]U. Scheithauer, G. Meyer, and M. Henzler, Surf. Sci. **178**, 441 (1986).
[28]H.-N. Yang, T.-M. Lu, and G. C. Wang, Phys. Rev. Lett. **62**, 2148 (1989).

[29]H.-N. Yang, T.-M. Lu, and G.-C. Wang, Phys. Rev. Lett. **63**, 1621 (1989).
[30]H.-N. Yang, T.-M. Lu, and G.-C. Wang, Phys. Rev. B **43**, 4714 (1991).
[31]H.-N. Yang, K. Fang, T.-M. Lu, and G.-C. Wang, Phys. Rev. B **44**, 1306 (1991).
[32]C. Kroll, M. Abraham, and W. Göpel, Surf. Sci. **253**, 157 (1991).
[33]Y.-L. He, J.-K. Zuo, and G.-C. Wang, Surf. Sci. **254**, 21 (1991).
[34]W. Weiss, D. Schmeisser, and W. Göpel, Phys. Rev. Lett. **60**, 1326 (1988); Surf. Sci. **207**, 401 (1989).
[35]T.-M. Lu and M. G. Lagally, Surf. Sci. **120**, 47 (1982).
[36]M. Presicci and T.-M. Lu, Surf. Sci. **141**, 233 (1984).
[37]P. Fenter and T.-M. Lu, Surf. Sci. **154**, 15 (1985).
[38]J. M. Pimbley and T.-M. Lu, Surf. Sci. **159**, 169 (1985).
[39]C. S. Lent and P. I. Cohen, Surf. Sci. **139**, 121 (1984).
[40]P. R. Pukite, C. S. Lent, and P. I. Cohen, Surf. Sci. **161**, 39 (1985).
[41]J. Villain, D. R. Grempel, and J. Lapujoulade, J. Phys. F **15**, 809 (1985).
[42]U. Romahn, Ph.D. thesis, University of Karlsruhe (TH) (1992).
[43]N. M. Butt *et al.*, Acta Crystallogr. Sec. A **44**, 396 (1988).
[44]It is very difficult to determine the FWHM of a Lorentzian peak convoluted with a Gaussian if the width of the Lorentzian contributes with less than 10% to the measured peak width. The fit to the χ^2 as a function of the Gaussian width will not provide an absolute minimum. Therefore, one of the discrete values of the Gaussian width is taken as the resolution and the step width of the Gaussian FWHM is reflected in the deviation of the data points.
[45]E. G. McRae, T. M. Buck, R. A. Malic, and G. H. Wheatley, Phys. Rev. B **36**, 2341 (1987).
[46]H. van Beijeren and I. Nolden, in *Structures and Dynamics of Surfaces II,* edited by W. Schommers and P. von Blanckenhagen (Springer, Berlin, 1987), Chap. 7.5.2, p. 259, and references therein.
[47]J. W. M. Frenken, J. P. Toennies, and Ch. Wöll, Phys. Rev. Lett. **60**, 1727 (1988).